

## NUMERICAL STUDY OF THE THERMOSOLUTAL CONVECTION IN A 3-D CAVITY SUBMITTED TO CROSS GRADIENTS OF TEMPERATURE AND CONCENTRATION

by

**Meriem OUZAOUIT<sup>\*</sup>, Btissam ABOURIDA, Lahoucine BELARCHE,  
Hicham DOGHMI, and Mohamed SANNAD**

National School of Applied Sciences, Ibn Zohr University, Agadir, Morocco

Original scientific paper  
<https://doi.org/10.2298/TSCI170809070O>

*This study is a contribution to the numerical study of the thermosolutal convection in a 3-D porous cavity filled with a binary fluid submitted to cross gradients of temperature and concentration. The Navier-Stokes equations, mass and energy governing the physical problem are discretized by the finite volume method. The equations of conservation of momentum coupled with the continuity equation are solved using the SIMPLEC algorithm, then the obtained system is solved using the implicit alternating directions method. The numerical simulations, presented here, correspond to a wide range of thermal Rayleigh number ( $10^3 < Ra < 10^6$ ) and buoyancy ratio ( $1 < N < 12$ ). The Lewis and Prandtl numbers were fixed respectively at 5 and 0.71 and the sections dimension  $\varepsilon = D/H = 0.4$ . The temperature distribution, the flow pattern and the average heat and mass transfer are examined. The obtained results show significant changes in terms of heat and mass transfer, by proper choice of the governing parameters.*

Key words: porous cavity, 3-D cavity, cross gradients of temperature and concentration

### Introduction

Natural convection due to the double diffusion, is one of the most important thermal phenomenon frequently encountered in practical applications such as oceanography, the processes of drying, *etc.* The obvious interest of this kind of convection induced several theoretical and practical studies, considering the case of cross or parallel gradients of temperature and concentration. However a literature review showed that the majority of the available works considered the case of double 2-D diffusion [1-6], whereas the 3-D approach allows a better simulation of the flow and heat and mass transfers within the cavity [7, 8].

Hence, Beghein *et al.* [1] carried out a numerical study of the double diffusive natural convection in a square cavity submitted to horizontal temperature and concentration gradients. The purpose of their study was to determine the effect of the controlling parameters, such as Lewis number and the buoyancy ratio,  $N$ , on the fluid-flow. They noted the variation of the opposite  $N$  allowed a transitory behaviour of the flow. In addition, for a lower Lewis number  $Le = 1$  and for the opposite case ( $N < 0$ ) a strong diffusion of the pollutant is encountered in the cavity. However, when Lewis number is much larger than the unit, the pollutant is found to be very concentrated in a very thin boundary-layer, while the core of the cavity is filled with homogeneous fluid.

<sup>\*</sup>Corresponding author, e-mail: meriem.ouzaouit@gmail.com

A 2-D numerical study of the thermosolutal convection in a square cavity filled by water at around 4°C, heated by lower part and salted above is studied by Yoon *et al.* [2] to study the predominance of the solutal and thermal forces. Their results showed that the strong density, the temperature and concentration variations of the lower and higher wall and the controlling parameters have an important effect on the resulting oscillatory behaviours. Hence, the high density of water allows the appearance of a huge diffusion in favour of the natural convection. The increase of Rayleigh number generates also an oscillatory system of the flow. Oscillation of the fluid for a criticisms value of Grashof number decreases for ascending values of Lewis number and by the increase of the lower walls temperature.

On the other hand, some research considered the case of a rectangular cavity submitted to parallel or opposite temperature and concentration gradients. Hence, Akrouer *et al.* [3] conducted a numerical study on the double natural convection in a rectangular cavity with a vertical gradient of concentration and horizontal gradient of temperature. They studied the dominance of the thermal and solutal transfer and found that for  $N = 2$  and thermal Grashof varying between  $10^3$  and  $10^5$ , three modes of flow appear, two connectives cells due to the thermal force for small values of  $N$  and the flow dominated by the diffusion for great values of  $N$ . For a specific interval of  $N$  values, the transfer decreases when we increase  $N$ . In the transition zone, the solution depends essentially on the initial condition and an effect of hysteresis appears.

Benissaad *et al.* [4] carried out a numerical study of natural thermosolutal convection in a rectangular inclined cavity, filled with a porous media and saturated by a binary fluid. the vertical walls are submitted to variations of concentration and temperature, the horizontal walls are adiabatic and impermeable. This study was based on the effect of specific parameters on the flow and heat and mass transfer. The considered controlling parameters are the Darcy, Lewis, and Rayleigh numbers and the inclination angle of the enclosure. It was found that the intensity of the flow increased with the Darcy number while for lowest Darcy values, the porous media behaves like an impermeable wall. The growth of the flow intensity depends also on the number of Rayleigh and the Nusselt number decreased by increasing the Lewis number. This was linked by the authors to the increase of the mass forces and the reduction of the thermal ones.

For Younsi *et al.* [5], the temperature and concentration gradients were imposed horizontally. The model of Darcy-Brinkman-Forchheimer was used and leads to show that the heat and mass transfer and the flow field are deeply affected by the thermal and solutal buoyancy forces. Heat and mass transfers decrease with decreased permeability. Lee *et al.* [6] studied experimentally the stability of the double diffusion due to horizontal temperature and concentration gradients in a rectangular enclosure which different aspect ratio,  $A$ , varying between 0.2 and 2. The results show that for small and large values of  $N$  the flow is generated as unicellular. Whereas the multicellular mode of flow appears for  $8 < N < 55$  in the cooperating case and  $5 < N < 13$  in the opposing case.

A 3-D numerical study of the natural bidiffusive convection was developed by Sezai and Mohammad. [7]. They showed, in the case of a cubical enclosure with opposite and horizontally temperature and concentration gradients that the flow is strictly 3-D for certain values of the controlling parameters such as the buoyancy ratio, the thermal Rayleigh and the Lewis numbers. They observed the appearance of a secondary flow when  $N$  is increased and a variety complex flow patterns.

Benissaad *et al.* [8] studied the natural convection in a rectangular enclosure submitted to horizontal temperature and concentration gradient. Only the Grashof number was varied between  $10^4$  and  $10^7$ . The results showed that the flow is permanent for  $10^4 \leq Gr \leq 2.2 \times 10^5$  and  $6 \cdot 10^5 \leq Gr \leq 10^7$ . However, for  $3 \times 10^5 \leq Gr \leq 5 \cdot 10^5$ , the natural convection is transitory and

aperiodic. A decrease of the Nusselt number is observed for  $10^4 \leq Gr \leq 2.2 \cdot 10^6$ . While for  $Gr = 10^7$ , the Nusselt number grows regularly until 2.11. For  $10^4 \leq Gr \leq 10^5$ , a huge reduction the Sherwood number was encountered. In the transitory mode, the Sherwood number oscillates between 10.48 and 11.78.

The purpose of the present study is to simulate the 3-D natural convection due to double diffusion in cubical cavity submitted to cross concentration and temperature gradients. The effect of the variation of the controlling parameters on the heat and mass transfers is then developed.

### Problem description

The physical model, considered in this study, is illustrated in fig. 1. The geometry consists of a cubical cavity with height,  $H$ , and filled with a binary fluid. The left and right vertical walls, are maintained, respectively, to hot and cold temperatures ( $T_0 < T_1$ ) while the two other

vertical walls are partially submitted to a concentration gradient ( $C_0 < C_1$ ). The remaining walls are adiabatic, impermeable and no slip boundary conditions for all velocity components are adopted. The flow is considered laminar while the binary fluid is assumed to be Newtonian and incompressible. The Soret and Dufour effects are considered to be negligible and the fluid density constant, except in the buoyancy term of the Navier-Stokes equations, where it varies linearly with the local temperature and solutal mass fraction:

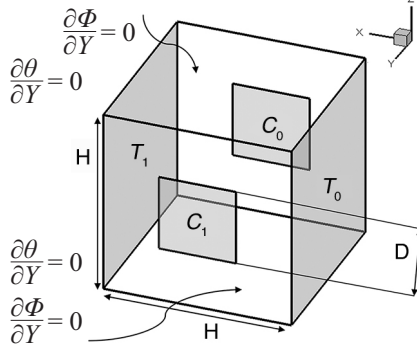


Figure 1. Studied configuration and co-ordinates

$$\rho = \rho_0 [1 - \beta_T (T - T_0) - \beta_C (C - C_0)] \quad (1)$$

$$\beta_T = -\frac{1}{\rho_0} \left[ \frac{\partial \rho}{\partial T} \right]_C, \quad \beta_C = -\frac{1}{\rho_0} \left[ \frac{\partial \rho}{\partial C} \right]_T \quad (2)$$

### Mathematical formulation

The thermophysical properties of the fluid are considered constant, and estimated at a reference temperature,  $T_{ref}$ , and solute mass fraction,  $C_{ref}$ . Adopting the following dimensionless variables:

$$\theta = \frac{T - T_{ref}}{T_1 - T_0}, \quad \Phi = \frac{C - C_{ref}}{C_1 - C_0}, \quad T_{ref} = \frac{T_1 + T_0}{2}, \quad C_{ref} = \frac{C_1 + C_0}{2} \quad (3)$$

The governing equations correspond to the conservation of mass, momentum, energy and concentration. Their no-dimensional form can be written:

$$\frac{\partial U}{\partial X} + \frac{\partial V}{\partial Y} + \frac{\partial W}{\partial Z} = 0 \quad (4)$$

$$\frac{\partial U}{\partial \tau} + U \frac{\partial}{\partial X} (U) + V \frac{\partial}{\partial Y} (U) + W \frac{\partial}{\partial Z} (U) = -\frac{\partial P}{\partial X} + \left( \frac{\partial^2 U}{\partial X^2} + \frac{\partial^2 U}{\partial Y^2} + \frac{\partial^2 U}{\partial Z^2} \right) \quad (5)$$

$$\frac{\partial V}{\partial \tau} + U \frac{\partial}{\partial X} (V) + V \frac{\partial}{\partial Y} (V) + W \frac{\partial}{\partial Z} (V) = -\frac{\partial P}{\partial Y} + \left( \frac{\partial^2 V}{\partial X^2} + \frac{\partial^2 V}{\partial Y^2} + \frac{\partial^2 V}{\partial Z^2} \right) \quad (6)$$

$$\frac{\partial W}{\partial \tau} + U \frac{\partial}{\partial X} (W) + V \frac{\partial}{\partial Y} (W) + W \frac{\partial}{\partial Z} (W) = -\frac{\partial P}{\partial Z} + \left( \frac{\partial^2 W}{\partial X^2} + \frac{\partial^2 W}{\partial Y^2} + \frac{\partial^2 W}{\partial Z^2} \right) + \frac{Ra}{Pr} (\theta + N\Phi) \quad (7)$$

$$\frac{\partial \theta}{\partial \tau} + U \frac{\partial \theta}{\partial X} + V \frac{\partial \theta}{\partial Y} + W \frac{\partial \theta}{\partial Z} = \frac{1}{\text{Pr}} \left( \frac{\partial^2 \theta}{\partial X^2} + \frac{\partial^2 \theta}{\partial Y^2} + \frac{\partial^2 \theta}{\partial Z^2} \right) \quad (8)$$

$$\frac{\partial \Phi}{\partial \tau} + U \frac{\partial \Phi}{\partial X} + V \frac{\partial \Phi}{\partial Y} + W \frac{\partial \Phi}{\partial Z} = \frac{1}{\text{Sc}} \left( \frac{\partial^2 \Phi}{\partial X^2} + \frac{\partial^2 \Phi}{\partial Y^2} + \frac{\partial^2 \Phi}{\partial Z^2} \right) \quad (9)$$

The parameters Ra, Pr, Sc, and  $N$  denote the Rayleigh number, Prandtl number, Schmidt number, and the buoyancy ratio, respectively. These parameters are defined:

$$\text{Ra} = \frac{g k \beta_T (T_1 - T_0) H^3}{\alpha \nu}, \text{Pr} = \frac{\nu}{\alpha}, \text{Sc} = \frac{\nu}{D}, N = \frac{\beta_c (C_1 - C_0)}{\beta_T (T_1 - T_0)} \quad (10)$$

The hydrodynamic boundary conditions are such as the velocity components are zero on the rigid walls of the enclosure ( $U = V = W = 0$ ). The dimensionless thermal and mass boundary conditions associated to the governing equations are:

- Lateral wall ( $X=0$ ):  $\theta_0 = -0.5$  and  $\partial \Phi / \partial X = 0$
- Lateral wall ( $X=1$ ):  $\theta_1 = 0.5$  and  $\partial \Phi / \partial X = 0$
- Lateral wall ( $Y=0$ ):  $\Phi_0 = -0.5$  across the section,  $\partial \Phi / \partial Y = 0$  else where on the wall,  $\partial \theta / \partial Y = 0$  over the entire wall
- Lateral wall ( $Y=1$ ):  $\Phi_1 = 0.5$  across the section,  $\partial \Phi / \partial Y = 0$  else where on the wall,  $\partial \theta / \partial Y = 0$ , over the entire wall

The local Sherwood number and the average Sherwood number, are respectively defined by:

$$\text{Nu}_{\text{loc}} = \frac{\partial \theta}{\partial X} \Big|_{X=0,1} \quad (11)$$

$$\text{Nu} = \int_0^1 \int_0^1 \text{Nu}(X, Y) \, dY \, dZ \quad (12)$$

$$\text{Sh}_{\text{loc}} = \frac{\partial \Phi}{\partial Y} \Big|_{Y=0,1} \quad (13)$$

$$\text{Sh} = \int_{0.3}^{0.7} \int_{0.3}^{0.7} \text{Sh}(X, Y) \, dY \, dZ \quad (14)$$

### Numerical formulation

The Navier-Stokes, energy and mass equations are discretized by the finite volume method developed by Patankar [9] using the power law scheme. The conservation equations of momentum coupled with the continuity equation are solved using the SIMPLEC algorithm. To solve the algebraic system obtained after discretization of the PDE, the implicit alternating directions method is used. The following criteria is applied to all dependent variables in each time step to ensure the convergence of the numerical algorithm:

$$\sum_{i,j,k=1}^{i_{\max} j_{\max} k_{\max}} \frac{|\Psi_{i,j,k}^{m+1} - \Psi_{i,j,k}^m|}{|\Psi_{i,j,k}^m|} \leq 10^{-4}$$

where  $\Psi$  represents a dependent variable  $U, V, W, P, T$ , and  $C$ . The indexes  $i, j, k$  indicate a grid point and the index  $m$  the current time at the finest grid level. A preliminary study of the effect of the grid has been conducted and allowed us to choose a uniform grid size of  $81 \times 81 \times 81$  as the most adequate for the present study. In fact, it gives a good compromise between the execution time and the accuracy of the convergence criteria and the maximum deviation remains within

0.5% when the grid was refined to  $121 \times 121 \times 121$ . The optimal time has also been found equal to  $10^{-4}$  after multiple tests. Finally, the accuracy of the numerical model was checked by comparing results from the present code with those previously published by Sezai and Mohamad [7] in the case of double diffusive natural convection in an enclosure. The resulting heat and mass transfer rates were found to be in excellent agreement with the reference, with maximum relative differences being less than 1.43% and 1.46% respectively for Nusselt and Sherwood numbers, tab.1.

**Table 1. Validation of the present code with the results of [7] for  $Pr = 10$ ,  $Ra = 10^5$  and different value of  $Le$**

Le	Nu [present study]	Sh [Present study]	Nu [7]	Sh [7]
0.5	3.32	1.91	3	1
1	3.9	3.9	3.9	3.9
2	4.11	5.94	4.11	5.6
5	4.12	8.05	4.25	8

## Results and discussion

The main parameters governing the present problem are the thermal Rayleigh number ( $10^3 < Ra < 10^5$ ) and the buoyancy forces ratio ( $1 < N < 12$ ). The Lewis number and the Prandtl number are fixed, respectively, at constant values equal to 5 and 0.71, respectively. The sections dimension,  $\varepsilon$ , is equal to 0.4.

### Effect of the governing parameters

In order to visualize the heat and mass transfer inside the cavity, fig. 2 shows the streamlines, isoconcentrations and isotherms for  $Ra = 10^5$ ,  $Pr = 0.71$ ,  $Le = 5$ ,  $\varepsilon = 0.4$ , and  $N = 8.5$  in different plans across the cavity ( $X = 0.5$ ,  $Y = 0.5$ , and  $Z = 0.5$ ).

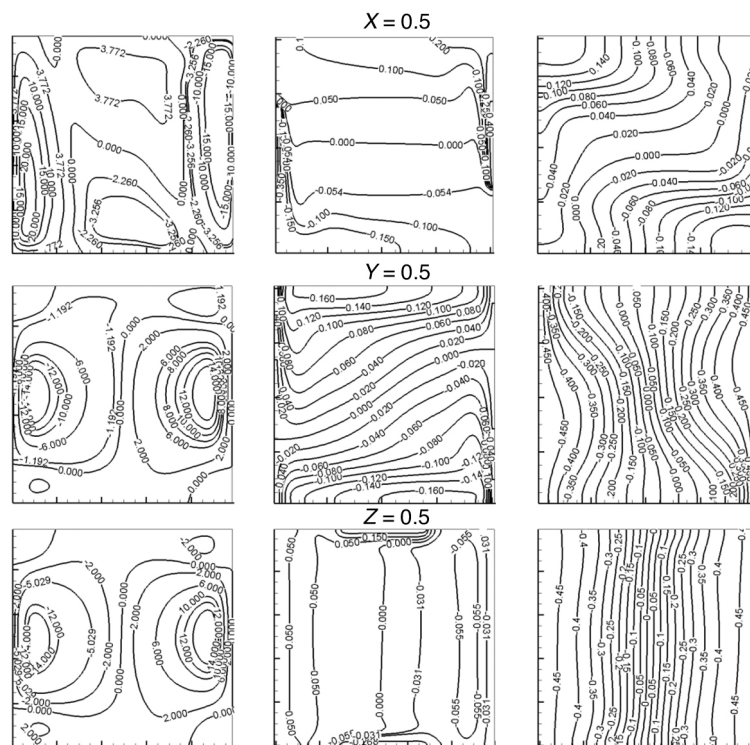


**Figure 2. Streamlines, isoconcentrations, and isotherms in the planes  $Z = 0.5$ ,  $Y = 0.5$ , and  $X = 0.5$  for  $Ra = 10^5$ ,  $Pr = 0.71$ ,  $Le = 5$  and  $N = 8.5$**



Indeed, a preliminary study was made for various ranges of the controlling parameters and a series of chosen plans in each of the three directions. This allowed us to choose the median plane  $Z = 0.5$ , as being the most representative with regards to the heat and mass exchanges within the cavity fig. 2. This plane was also found to be a symmetry plane of the flow and will be used here after for the presentation of the streamlines, isotherms and isoconcentration as shown in the fig. 3 for  $Ra = 10^5$ ,  $Pr = 0.71$ ,  $Le = 5$ ,  $\varepsilon = 0.4$  and different value of  $N$ .

The fig. 3, related to  $Z = 0.5$  plane, shows that the temperature and the concentration gradients induce complex fluid motion depending on the considered value of  $N$ .

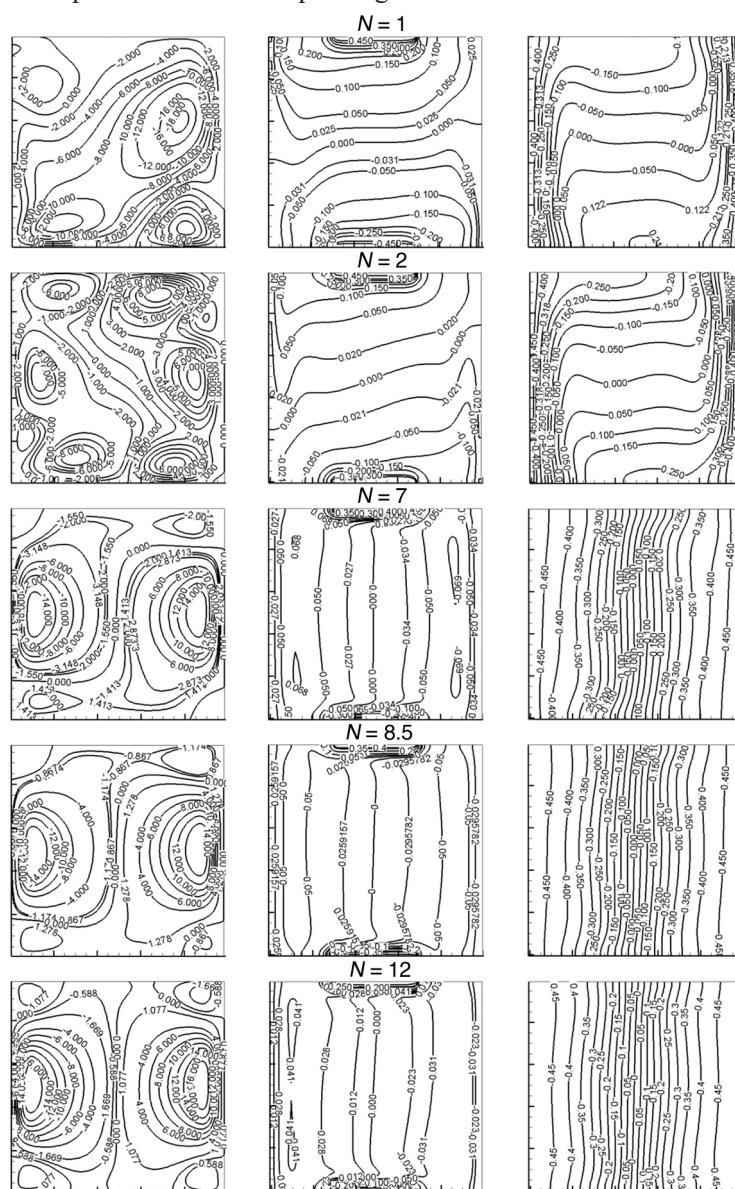
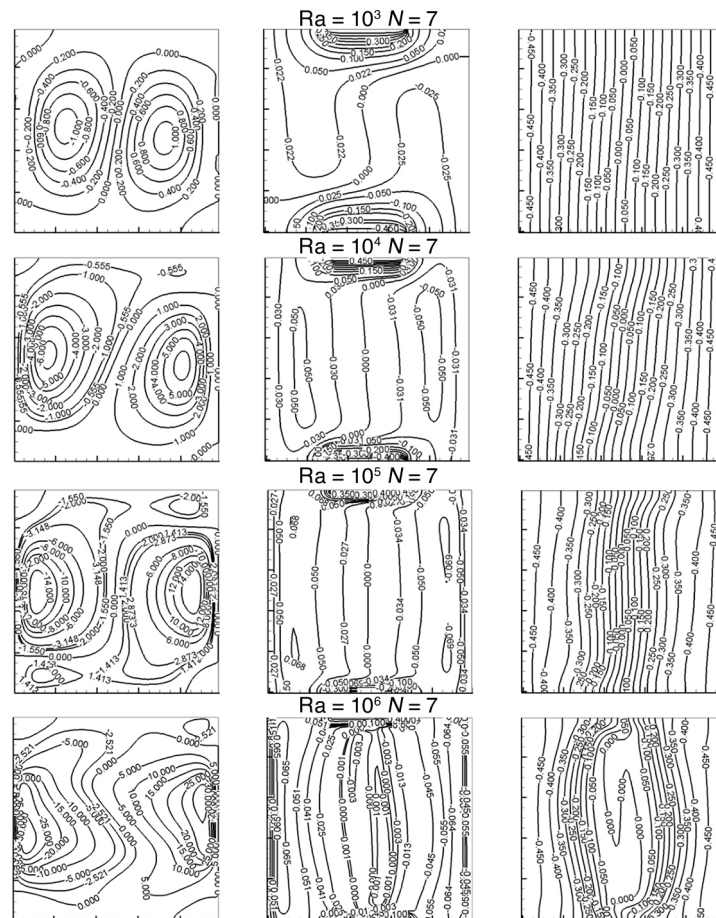


Figure 3. Streamlines, isoconcentrations, and isotherms  $Ra = 10^5$ ,  $Pr = 0.71$ ,  $Le = 5$ ,  $\varepsilon = 0.4$  and different  $N$

Hence, we can distinguish ever a flow regimes which depend on the value of  $N$ . In the case of  $N=1$  and  $N=2$ , the flow consists of a main cell and two small cells located in the upper and lower corners of the cavity and clockwise rotating. These cells starts to mix between them when  $N$  is increased ( $N=2$ ). The thermal fields variations, corresponding to  $N=1$  and  $N=2$ , are maintained by the flow motion from the right side of the cavity.

However, horizontal stratification of the isotherms appears in the center of the cavity for  $N=1$ , reflecting homogeneous and stable temperature fields. The horizontal temperature stratification starts to change for  $N=2$  to announcing a change in the heat transfer behavior. The figures show also a limited distribution of the concentration with a stratification in the center of the cavity for  $N=1$ .



**Figure 4.** Streamlines, iso-concentration, and isotherms in the plane  $Z=0.5$ ,  $Pr=0.71$ ,  $Le=5$ ,  $N=7$  and different  $Ra$

The isoconcentrations are more tight near the horizontal walls indicating a good mass transfer from the higher concentration wall towards the lower one. However, by increasing  $N$  ( $N=2$ ), an horizontal deformation appears in the center of the cavity.

In the case of  $2 < N < 12$ , the increase of  $N$  makes it possible to enhance the concentration gradient within the cavity and create a strong buoyancy force involving a rotary fluid

movement in the plane  $X$ - $Y$ . The flow in this case consists of two large counter-rotating cells, occupying most of the cavity with small recirculation cells located in the left and right corners. A further increase of the buoyancy ratio induces a higher intensity of the main cells and the appearance of small recirculation cells in the corners.

On the other hand, when  $N$  is increased from 2 to 7, we can notice the vertical stratification of the temperature fields, from the hot walls towards the cold one.

However, these fields does not undergo any noticeable deformation for further increase of  $N$ . This shows the dominance of the mass transfer compared to the thermal one.

The concentration fields show clearly the effect of  $N$ . Hence for  $N$  higher than 2, the isoconcentrations show a vertical stratification. For a further increase of  $N$ , the concentration gradients becomes weak on the top and bottom horizontal walls and more stratified on the left and right vertical walls which explains a very important mass transfer within the cavity.

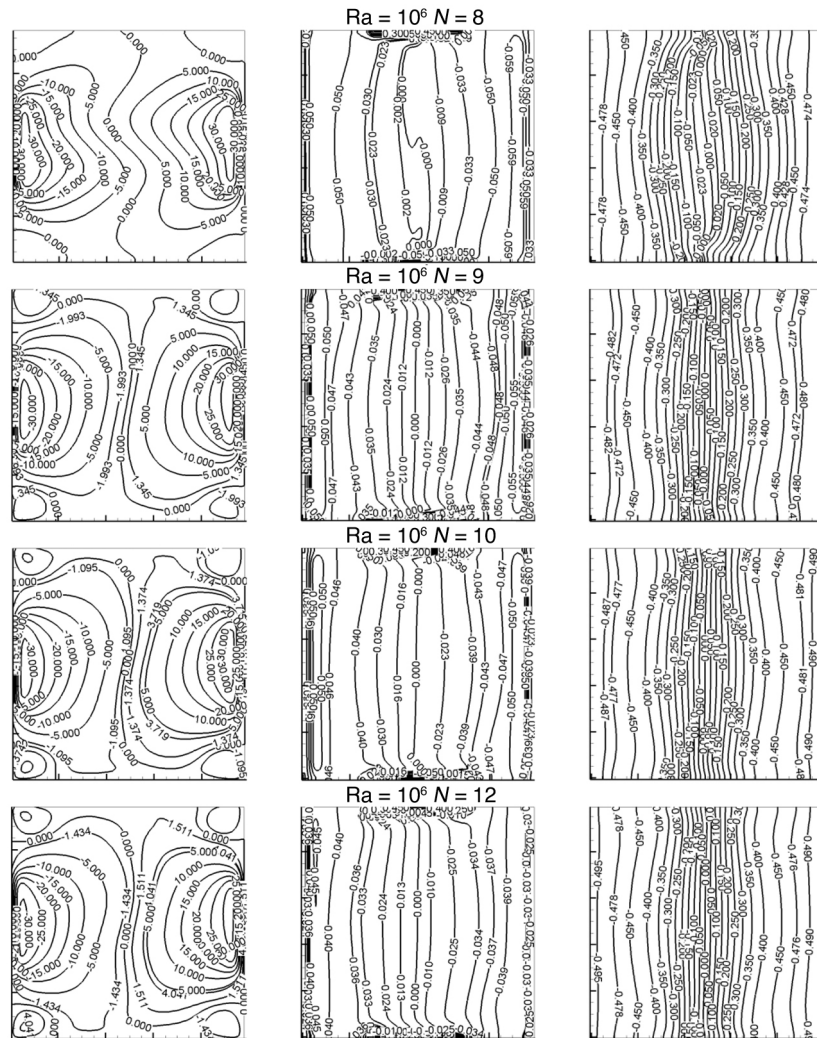


Figure 5. Streamlines, iso-concentration, and isotherms in the plane  $Z = 0.5$ ,  $Pr = 0.71$ ,  $Le = 5$ ,  $Ra = 10^6$  and different  $N$



In fig. 4, the thermal Rayleigh number is varied between  $10^3$  and  $10^6$  for  $N=7$  and  $Le=5$ . For  $Ra = 10^3$  and  $10^4$ , the fluid-flow consists of two counter-rotating symmetrical cells. For  $Ra = 10^3$ , the boundary-layers are very thin in the vicinity of the active walls and becomes thicker progressively far from the walls indicating a good heat transfer from the hot wall to the cold one. The isotherms show a stratification in the  $Z = 0.5$  plane, which denotes a dominant conductive heat transfer within the cavity. For  $Ra = 10^4$ , the isotherms show similar structure as those corresponding to  $Ra = 10^3$  with a small deformation in the centre announcing the beginning of the convective mode. The concentration gradients are located near the horizontal walls, which indicates a good mass transfer within the cavity. For these two values of Rayleigh number, the isoconcentrations undergo weak deformation in the centre of the cavity while the main transfer occurs near the left and right walls.

For  $Ra = 10^5$ , the fluid-flow consists of two rotating cells located in the center and two other small ones in the sides of the cavity. The isotherms are no longer parallel, but undergo a small deformation in the middle and the corner of the cavity and begins to be more tight. The isoconcentration obtained for  $Ra = 10^5$  are stratified, horizontally parallel and very tight near of the sources.

However, for  $Ra = 10^6$  and  $N=7$ , the two large cells became deformed in the center. the shape of the isotherms indicates a stronger convection mode. The isoconcentrations are also tight in the walls vicinity and forms a very small vortex in the middle of the cavity due to the effect of high Rayleigh number.

Figure 5. also shows the isotherms and isoconcentrations in the middle  $XY$  plane for  $Ra = 10^6$  and different values of  $N$  (8, 9, 10, 12). We can notice that for  $N=8$ , the flow is characterized with two central deformed vortexes. The isotherms and isoconcentrations are distorted in the center of the cavity and vertical near the active walls promote the convective mode. For  $N=9, 10$ , and  $12$ , the fluid undergoes almost the same changes, the stream lines appear in the forms of two large cells in the center with four small vortexes in the corners. The isoconcentrations and isotherms are slightly deformed and tight in the center and in the walls vicinity. We can notice that since  $N=9$  and for higher values of  $N$ , the fluid-flow shows the same permanent shape.

Figure 6 comes to support the results found in the figs. 3-5. It represents the effect of  $N$  on the Nusselt and Sherwood numbers characterizing, respectively, the heat and mass transfers. We can notice the increase of Sherwood number and the diminution of Nusselt number with  $N$  until reaching constant values from  $N=7$ . Hence, the increase of  $N$  induces a stronger mass convection and a diminution of the heat transfer until stabilization.

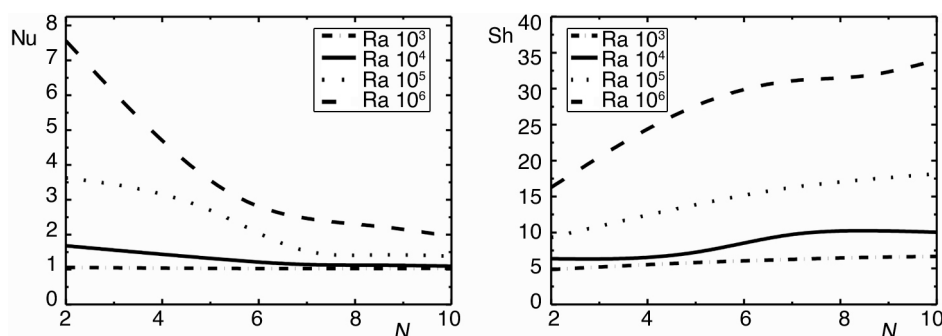


Figure 6. Variation of Nusselt and Sherwood numbers with  $N$  for  $Pr = 0.71$ ,  $Le = 5$ ,  $\varepsilon = 0.4$ , and different  $Ra$

Figure 6 presents also the effect of the thermal Rayleigh number on Nusselt and Sherwood numbers. For low values of Rayleigh,  $Ra = 10^3$  and  $10^4$ , the heat transfer is very weak and almost constant as shown by the Nusselt values. For  $Ra = 10^6$  and  $10^5$ , the increase of the convective effects leads to ascending values of Nusselt number. In addition, the Sherwood number continues to increase with Rayleigh number with dominant mass forces and reaches bigger values for  $Ra = 10^6$ , showing the evident effect of the Rayleigh number on the mass transfer.

## Conclusion

In this work, we studied a numerical 3-D simulation of the natural double-diffusion in a cubical enclosure subjected to cross gradients of temperature and concentration. The obtained results show that:

- The variation of the buoyancy ratio  $N$  ( $2 \leq N \leq 12$ ) show that since  $N \geq 2$ , the isoconcentrations undergo a clear deformation whereas the isotherms remain almost unchangeable even when considering different Rayleigh numbers.
- The increase of Rayleigh number induces a strong growth of Sherwood number and Nusselt number for the considered range of  $N$ . However when  $N$  is increased above 7, the resulting fluid flow does not show big changes which induces a weaker variation for Nusselt number and Sherwood number. Hence, the resulting Nusselt and Sherwood numbers depend strongly on the considered values of Rayleigh number and  $N$ .

## Nomenclature

$A$	– aspect ratio	$u, v, w$	– velocity component [ $\text{ms}^{-1}$ ]
$d$	– mass diffusivity, [ $\text{m}^2\text{s}^{-1}$ ]	$U, V, W$	– dimensionless velocity
$D$	– the sections' height	$x, y, z$	– cartesian co-ordinates, [m]
$g$	– acceleration of gravity [ $\text{ms}^{-2}$ ]	$X, Y, Z$	– dimensionless co-ordinates
$Gr$	– Grashof number	<i>Greek symbols</i>	
$H$	– cavity height, [m]	$\alpha$	– thermal diffusivity, [ $\text{m}^2\text{s}^{-1}$ ]
$k$	– thermal conductivity [ $\text{Wm}^{-1}\text{K}^{-1}$ ]	$\beta_T$	– thermal expansion coefficient
$Le$	– Lewis number	$\beta_c$	– mass expansion coefficient
$N$	– buoyancy ratio	$\varepsilon$	– the sections' dimension
$Nu$	– Nusselt number	$\theta$	– dimensionless temperature
$P$	– pressure [ $\text{Nm}^{-2}$ ]	$\mu$	– dynamic viscosity, [ $\text{kgms}^{-1}$ ]
$Pr$	– Prandtl number	$\rho_0$	– mass density, [ $\text{kgm}^{-3}$ ]
$Ra$	– Rayleigh number	$\nu$	– kinematic viscosity [ $\text{m}^2\text{s}^{-1}$ ]
$Sc$	– Schmidt number	$\Phi$	– dimensionless concentration
$Sh$	– Sherwood number	<i>Subscript</i>	
$T$	– temperature, [K]	loc	– local

## References

- [1] Beghein, C., *et al.*, Numerical Study of Double-Diffusive Natural Convection in a Square Cavity, *Int. J. Heat Mass Transfer* 35 (1992), 4, pp. 833-846
- [2] Yoon, J., *et al.*, Transient Thermo-Solutal Convection of Water Near 4 °C With Opposing Gradients in a Square Cavity, *International Journal of Heat and Mass Transfer* 52 (2009), 21-22, pp. 4835-4850
- [3] Akrou, D., *et al.*, Unsteady Flow Study in Double Diffusion with Opposite Temperature and Concentration Gradient, *Rev. Energ. Ren.: Chemss* 2000 pp. 99-104
- [4] Benissaad, S., *et al.*, Thermosolutal Convection Study in an Inclined Enclosure, *Proceedings, International Seminar on Mechanical Technologies, SITEM'2009*, Abou-Beker Belkaid University, Tlemcen, Algeria, 2009
- [5] Younsi, R., *et al.*, Numerical Simulation of Double-Diffusive Natural Convection in Porous Cavity: Opposing flow. *The Arabian Journal for Science and Engineering*, 27 (2002), 1C, pp 181-194

- [6] Lee, J., *et al*, Natural Convection in Confined Fluids With Combined Horizontal Temperature and Concentration Gradients, *Int. J. Heat Mass Transfer* 31 (1988), 10, pp. 1969-1977
- [7] Sezai, I., Mohamad, A., Double Diffusive Convection in a Cubic Enclosure With Opposing Temperature and Concentration Gradients, *Phys. Fluids* 12 (2000), 9, 2210
- [8] Benissaad, S., *et al* , Numerical Study of Three-Dimensiona Opposing Natural Thermosolutal Convection, *The Bulletin of the Polytecnic Institute of Jassy, Construction. Architecture Section*, 64 (2006), 4, pp. 109-124
- [9] Patankar, S.V., *Numerical Heat Transfer and Fluid Flow*, McGraw-Hill, New York, USA, 1980